Forced Convection Boundary Layer Flow along a Horizontal Cylinder in Porous Medium Filled by Nanofluid

Azizah. Mohd Rohni, Syakila. Ahmad, and Ioan. Pop

***Abstract*—**The problem of steady axisymmetric forced convection boundary layer flow past a horizontal circular cylinder placed in porous medium filled with copper (Cu) – water, alumina (Al2O3) – water and titania (TiO2) – water nanofluid has been studied numerically in this paper. The system of partial differential equations is transformed into ordinary differential equations using appropriate transformations and then solved numerically using shooting method through shootlib function from maple software. Numerical results are obtained for the local Nusselt number as well as for the temperature profiles for some values of the governing parameters, namely, the nanoparticle volume fraction parameter ϕ and the curvature parameter γ. It is shown that the presence of nanoparticle in the base fluid would increase the heat transfer characteristics. It is also found that heat transfer characteristics increase with increasing nanoparticle volume fraction and curvature parameters.

***Keywords*—**Forced convection, horizontal circular cylinder, nanofluid, porous medium.

I. Introduction

CONVECTIVE flow in fluid-saturated porous media has been extensively studied due to a wide range of geophysical and engineering applications including geothermal energy extraction, ground water resource management, building thermal insulation, enhanced oil recovery, nuclear waste disposal, metal casting (alloy solidification), grain storage, and heat transfer in electronic equipment, among many others. An enormous literature review on this subject can be found in the recent books by [1] and [2]. The problem of forced convection boundary layer flow of regular fluids past a cylinder embedded in a porous medium was previously studied in different ways. Representative studies can be found in by [3], [4] and [5]. In contrast, there is still no study extended the mentioned problem to the nanofluids.

Azizah. Mohd Rohni is with School of Mathematical Sciences, Universiti Sains Malaysiat, 11800 USM Penang, Pulau Pinang, Malaysia. (corresponding author's phone:+6049286885; fax:+6049286906 ; e-mail: azizahrohni@yahoo.com).

Syakila. Ahmad, was with School of Mathematical Sciences, Universiti Sains Malaysiat, 11800 USM Penang, Pulau Pinang, Malaysia (e-mail: syakila.ahmad@ymail.com).

Ioan. Pop is with Faculty of Mathematics, university of Cluj, R-3400 Cluj, CP253, Romania. (e-mail: popm.ioan@yahoo.co.uk).

Meanwhile, nanofluids itself was first introduced by [6] in order to develop advanced heat transfer fluids with substantially higher conductivities. The resulting mixture of nanoparticles and the base fluid possess unique physical and chemical properties which can enhance the phenomenon of heat transfer. Recently, nanofluids have the application in the gas and oil industries whereas nanoparticles in nanofluids can flow through permeable media, thus improve oil recovery. Nanofluids also can be used for improving oil recovery particularly for viscous oils where usually a fluid such as water is injected into the porous medium to displace the oil, as the viscosity of water is often less than the oil. However, increasing the viscosity of the injected fluid for example by using nanofluids would significantly increase the recovery efficiency [7].

The nanoparticles used in nanofluids are typically made of metals (Al, Cu), oxides (Al_2O_3, TiO_2 and CuO), nitrides (AIN, SiN) or nonmetals (graphite, carbon nanotubes) and the base fluid is usually a conductive fluid, such as water, ethylene glycol or engine oil (see [8] and [9]). The thermal conductivity enhancement of nanofluids is shown by [10] to be depended on the volume fraction of the suspended particles and the thermal conductivities of the particles and base fluids. There are many studies on the mechanism behind the enhanced heat transfer characteristics utilising nanofluids and they may be found in [11] – [20]. However, none of these studies in nanofluid so far, considered the problem of forced convection boundary layer flow past a horizontal circular cylinder embedded in a porous medium.

Therefore, in this paper, we try to make an attempt to investigate theoretically the problem of steady forced convection boundary layer flow past a horizontal circular cylinder embedded in porous media filled with nanofluid whereas the water based nanofluid containing three different types of nanoparticles: copper (Cu), alumina (Al_2O_3) and titania (TiO_2). The objective of this paper is to study the influence of nanoparticle volume fraction and curvature parameters to the thermal characteristics in three different types of nanofluid. To the authors' present knowledge, this study has not been conducted earlier in literature and it is hoped that the results obtained will contribute towards better understanding about the thermal characteristics in nanofluid.

II. MATHEMATICAL ANALYSIS

Consider the steady, axisymmetric boundary layer flow along a horizontal circular cylinder of radius a which is embedded in a porous medium filled with nanofluids. It is assumed that the velocity of the outer (potential) flow $u_e(x)$ and the surface temperature $T_w(x)$ are of the form $u_e(x) = U_0(x/a)$ and $T_w(x) = T_\infty + T_0(x/a)$ respectively, where U_0 and T_0 are constants with $U_0 > 0$ and $T_0 > 0$ (heated cylinder). The physical situation and coordinate system of the problem considered is shown in Fig. 1.

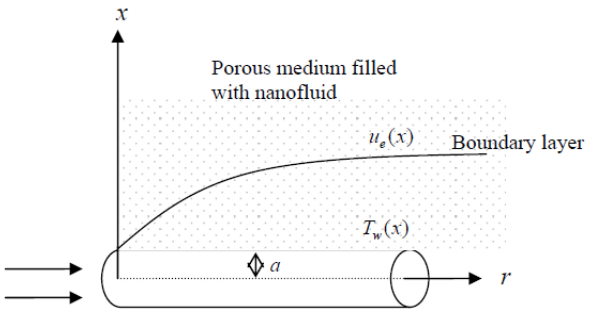

Fig. 1 Physical situation and coordinate system

Under these assumptions and based on Darcy's law, following [1] and along with the Boussinesq and boundary layer approximations, together with using the nanofluid model proposed by [15], the basic equations are

$$\frac{\partial}{\partial x}(ru) + \frac{\partial}{\partial r}(rv) = 0 \tag{1}$$

$$u = U_0(x/a) \tag{2}$$

$$u\frac{\partial T}{\partial x} + v\frac{\partial T}{\partial r} = \frac{\alpha_{nf}}{r}\frac{\partial}{\partial r}\left(r\frac{\partial T}{\partial r}\right) \tag{3}$$

subject to the boundary conditions

$$\begin{aligned} &v = 0, \quad T = T_w(x) = T_\infty + T_0(x/a) \quad \text{at} \quad r = a \\ &T = T_\infty \quad \text{as} \quad r \to \infty \end{aligned} \tag{4}$$

Here x and r are the cylindrical coordinates measured along the axis of the cylinder and normal to the surface of the cylinder in the radial direction respectively, u and v are the velocity components along x and r axes, respectively, T is the temperature of the nanofluid, φ is the nanoparticle volume fraction, β_f and β_s are the coefficients of thermal expansion of the fluid and of the solid, respectively, ρ_f and ρ_s are the densities of the fluid and of the solid fractions, respectively, μ_{nf} is the viscosity of the nanofluid and α_{nf} is the thermal diffusivity of the nanofluid, which are given by

$$\mu_{nf} = \frac{\mu_f}{(1-\varphi)^{2.5}}, \quad \alpha_{nf} = \frac{k_{nf}}{(\rho C_p)_{nf}}, \quad (\rho C_p)_{nf} = (1-\varphi)(\rho C_p)_f + \varphi(\rho C_p)_s \tag{5}$$

$$\frac{k_{nf}}{k_f} = \frac{(k_s + 2k_f) - 2\varphi(k_f - k_s)}{(k_s + 2k_f) + \varphi(k_f - k_s)}$$

where μ_f is the dynamic viscosity of the base fluid and its expression has been proposed by [19], k_{nf} is the thermal conductivity of the nanofluid, k_f and k_s are the thermal conductivities of the base fluid and of the solid, respectively, and $(\rho C_p)_{nf}$ is the heat capacitance of the fluid nanofluid. It is worth mentioning that the expressions (5) are restricted to spherical nanoparticles where it does not account for other shapes of nanoparticles. Equations (5) were also used by [15], [17] and [18].

Equations (1) – (3) can be transformed into the corresponding ordinary differential equations by the following transformation (see [20])

$$\eta = \frac{r^2 - a^2}{2\alpha_f a}\left(\frac{U_0\alpha_f}{2a}\right)^{1/2}, \quad \psi = \left(2U_0 a\alpha_f\right)^{1/2} x f(\eta), \quad \theta(\eta) = \frac{T - T_\infty}{T_w - T_\infty} \tag{6}$$

where ψ is the stream function, which is defined as $u = r^{-1}\partial\psi/\partial r$ and $v = -r^{-1}\partial\psi/\partial x$. Using (6), Eqs. (2) and (3) reduce to the following ordinary differential equations

$$f' = 1 \tag{7}$$

$$\frac{k_{nf}/k_f}{(1-\phi) + \phi(\rho C_p)_s/(\rho C_p)_f}\left[(1 + 2\gamma\eta)\theta'' + 2\gamma\theta'\right] + 2f\theta' - 2f'\theta = 0 \tag{8}$$

subject to the boundary conditions

$$\begin{aligned} &f(0) = 0, \quad \theta(0) = 1 \\ &\theta(\eta) \to 0 \quad \text{as} \quad \eta \to \infty \end{aligned} \tag{9}$$

Here prime denotes differentiation with respect to η, and the constants γ is the curvature parameter, which are defined by

$$\gamma = \left(\frac{\alpha_f}{U_0 a}\right)^{1/2} \tag{10}$$

Integrating Eq. (7) subject to boundary conditions (9) yields

$$f(\eta) = \eta \tag{11}$$

Substituting Eq. (7) and Eq. (11) into Eq. (8) and applying boundary condition (9) gives

$$\frac{k_{nf}/k_f}{(1-\phi) + \phi(\rho C_p)_s/(\rho C_p)_f}\left[(1 + 2\gamma\eta)\theta'' + 2\gamma\theta'\right] + 2\eta\theta' - 2\theta = 0 \tag{12}$$

with corresponding boundary conditions

$$\begin{aligned} &\theta(0) = 1 \\ &\theta(\eta) \to 0 \quad \text{as} \quad \eta \to \infty \end{aligned} \tag{13}$$

The physical quantity of interest is the local Nusselt number Nu_x, which is defined as

$$Nu_x = \frac{x q_w}{k_f (T_w - T_\infty)} \tag{14}$$

where the heat transfer from the cylinder q_w are given by

$$q_w = -k_{nf}\left(\frac{\partial T}{\partial r}\right)_{r=a} \tag{15}$$

Using the similarity variables (6), we get

$$(Pe_x / 2)^{-1/2} Nu_x = \frac{k_{nf}}{k_f}\left[-\theta'(0)\right] \tag{16}$$

where $Pe_x = u_e(x)\, x / \alpha_f$ is the local Péclet number.

III. METHOD OF SOLUTION

The boundary value problem of Eq. (12) subject to boundary conditions (13) is solved via shooting technique by converting it into an equivalent initial value problem. Therefore, we set

$$\theta' = \theta_p, \quad \frac{k_{nf}/k_f}{(1-\phi)+\phi(\rho C_p)_s/(\rho C_p)_f}\left[(1+2\gamma\eta)\theta_p' + 2\gamma\theta_p\right] + 2\eta\theta_p - 2\theta = 0 \tag{17}$$

with the boundary conditions

$$\theta(0) = 1, \quad \theta_p(0) = \beta \tag{18}$$

In order to integrate Eq. (17) as an initial value problem, we require a value for $\theta_p(0)$ i.e. $\theta'(0)$. Since this value is not given in the boundary conditions (18), a suitable guess values for $\theta'(0)$ are made and integration is carried out. Then, we compare the calculated values for $\theta(\eta)$ at η_∞ with the given boundary conditions $\theta(\eta_\infty) = 0$ and adjust the estimated values, $\theta'(0)$ and η_∞ to give a better approximation for the solution. This computation is done with the aid of shootlib function in Maple software.

IV. RESULTS AND DISCUSSION

The numerical computations using shooting method with the aid of shootlib function in Maple software have been carried out and results are reported for three different types of nanofluids, viz.: copper-water, alumina-water and titania-water as working fluids with different value of nanoparticle volume fraction ϕ and curvature γ parameters. It is worth to highlight that following [15], the values of ϕ considered are $0 \le \phi \le 0.2$. Therefore, we chose ϕ = 0.0 (regular fluid), 0.05, 0.1 and 0.2. The thermophysical properties of fluid and nanoparticles is given in Table 1.

In Table 2, the results of local Nusselt number $(k_{nf}/k_f)\left[-\theta'(0)\right]$ are presented for the chosen values of ϕ and γ . Further, to give a physical insight, the results in Table 2 are plotted in Fig. 2. From both Table 2 and Fig. 2, it is clear that, the inclusion of nanoparticle i.e. copper, alumina and titania respectively with $0 < \phi \le 0.2$ can enhance heat transfer behaviour compare to regular fluid ($\phi = 0$) and it becomes more pronounced with the increase of the nanoparticle volume fraction. It is also clear that local Nusselt number for cylinder ($\gamma \ne 0$) is higher compare to flat plate (γ = 0) and it continues to increase with increasing curvature parameter γ. The difference in local Nusselt number for three different nanoparticles can be obviously observed for higher curvature parameter γ. It is found that for every curvature γ and nanoparticle volume fraction ϕ parameters chosen, copper gives the highest Nusselt number followed by alumina and titania. This is due to copper has the highest thermal conductivity among them as can be seen in Table 1.

Moreover, in Fig. 3 temperature profiles for titania-water working fluid are depicted. This is to show how the mixture of nanoparticle with the base fluid alters the temperature characteristics compare to the base fluid alone. It is clear that for every curvature parameter γ, the presence of titania nanoparticle in the base fluid (denoted by dash line) increase the temperature profile compare to the base fluid alone (denoted by solid line). As happened in local Nusselt number, temperature profiles for cylinder ($\gamma \ne 0$) is higher compare to flat plate ($\gamma = 0$) and for cylinder itself, the temperature increases with increasing curvature parameter γ.

Finally, Fig. 4 illustrates the temperature profiles for three different nanofluid when ϕ = 0.2. Among the three different nanofluid considered, for both $\gamma = 3$ and $\gamma = 10$, titania-water working fluid has the smallest temperature profile whilst copper-water and alumina-water working fluid, respectively has almost the same temperature profiles where both overlap with one another. Therefore, in Fig. 4, although there actually three curves exist for each curvature parameter $\gamma = 3$ and $\gamma = 10$, but it is seen only two curves appear for $\gamma = 3$ and $\gamma = 10$ respectively. This is because the curves representing copper-water and alumina-water working fluid are redundant.

V. CONCLUSIONS

In this paper, we have numerically studied the problem of forced convection boundary layer flow along an axisymmetric horizontal circular cylinder embedded in porous medium filled with nanofluid. The governing boundary layer equations have been transformed to ordinary differential equations using similarity transformation. The resulting similarity equations have been solved using shooting method. The influence of different types of nanoparticle (copper, alumina and titania), nanoparticle volume fraction and the curvature parameter on the heat transfer characteristics have been examined. These characteristics are showed by the values of the local Nusselt number and temperature profiles. From this study, we could draw the following conclusions:

- The presence of nanoparticle in the base fluid enhances the heat transfer rate and temperature profiles.
- For all types of nanofluid that have been considered, i.e. copper-water, alumina-water and titania-water, the heat transfer rate increases with increasing nanoparticle volume fraction parameter and curvature parameter .
- For every curvature parameter considered, copper-water working fluid has the highest heat transfer rate followed by alumina-water and titania-water working fluid.
- The inclusion of copper and alumina nanoparticles, respectively, into the base fluid gives almost the same temperature profiles and they are higher compare to the temperature profiles for the suspension of alumina in the base fluid.

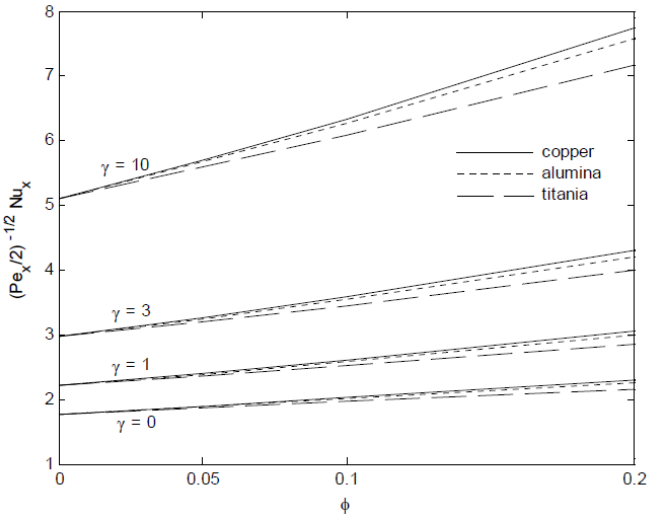

Fig. 2 Variation of the local Nusselt number with ϕ for different values of the curvature parameter γ .

TABLE I
THERMOPHYSICAL PROPERTIES OF FLUID AND NANOPARTICLES (SEE [15]).

Physical properties	Fluid phase (water)	copper	alumina	titania
C_p (J/kg K)	4179	385	765	686.2
ρ (kg/m^3)	997.1	8933	3970	4250
k (W/mK)	0.613	400	40	8.9538

TABLE II
LOCAL NUSSELT NUMBER OF NANOFLUIDS FOR DIFFERENT NANOPARTICLE VOLUME FRACTION AND CURVATURE PARAMETER

		$\frac{k_{nf}}{k_f}[-\theta'(0)]$		
γ	ϕ	copper	alumina	titania
0	0.0	1.7725	1.7725	1.7725
	0.05	1.8983	1.8882	1.8684
	0.1	2.0274	2.0062	1.9655
	0.2	2.3006	2.2532	2.1655
1	0.0	2.2117	2.2117	2.2117
	0.05	2.4040	2.3910	2.3618
	0.1	2.6063	2.5788	2.5174
	0.2	3.0513	2.9880	2.8502
3	0.0	2.9650	2.9650	2.9650
	0.05	3.2649	3.2471	3.2025
	0.1	3.5844	3.5461	3.4515
	0.2	4.2962	4.2067	3.9913
10	0.0	5.1114	5.1114	5.1114
	0.05	5.7038	5.6723	5.5858
	0.1	6.3376	6.2693	6.0854
	0.2	7.7525	7.5903	7.1704

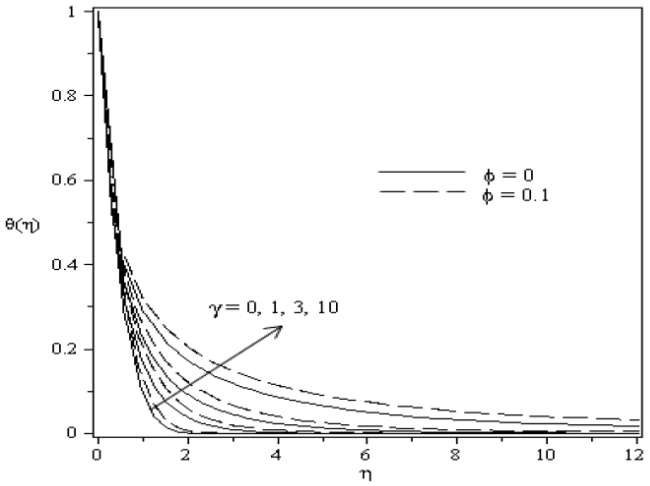

Fig. 3 Temperature profiles for TiO2 with different curvature parameter γ .

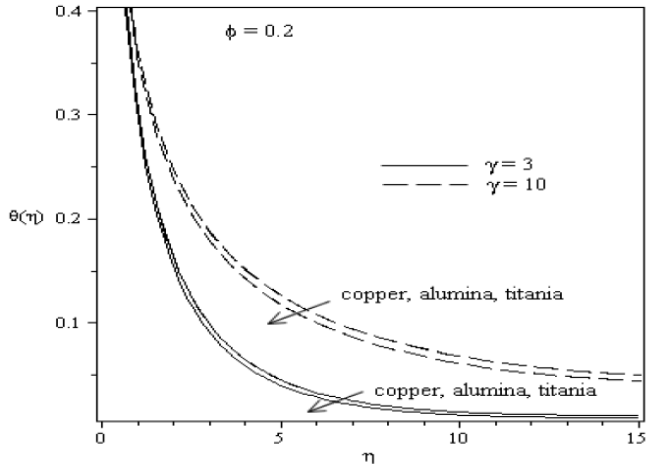

Fig. 4 Temperature profiles for three different types of nanofluids with ϕ = 0.2 and γ = 3 and 10.

ACKNOWLEDGMENT

The authors gratefully acknowledge the financial supports received in the form of research grants: Incentive Grant and Research University Grant (1001/PMATHS/811166) from Universiti Sains Malaysia. The first author would like to acknowledge Universiti Utara Malaysia and Ministry of Higher Education, Malaysia for the financial support received throughout the course of this study.

REFERENCES

[1] D.A. Nield and A. Bejan, *Convection in Porous Media*, 3rd edn. Springer, New York, 2006.

[2] D.B. Ingham and I. Pop. *Transport Phenomena in Porous Media*, Elsevier, London, 2005.

[3] R. Vasantha, G. Nath and I. Pop, Forced convection along a longitudinal cylinder embedded in a saturated porous medium, *Int. Comm. Heat Mass Transfer*, 14, pp. 639 – 646, 1987.

[4] S. Kimura, Forced convection heat transfer about a cylinder placed in porous media with longitudinal flows, *Int. J. Heat Fluid Flow*, 9, pp.83 – 86, 1988.

[5] E. Magyari, B. Keller and I. Pop, Exact analytical solutions of forced convection flow in a porous medium, *Int. Comm. Heat Mass Transfer*, 28, pp. 233 – 241, 2001.

[6] S.U.S. Choi, Enhancing thermal conductivity of fluids with nanoparticles, *ASME Fluids Eng. Division*, 231, pp. 99-105, 1995.

[7] M. Memari, A. Golmakani and A. M. Dehkordi, Mixed convection flow of nanofluids and regular fluids in vertical porous media with viscous heating, Industrial & Engineering Chemistry Research, 50 , pp. 9403 – 9414, 2011.

[8] X.Q. Wang, A.S. Mujumdar, A review on nanofluids – Part I: Theoretical and numerical investigations *Brazilian J. Chem. Engng*, 25, pp. 613-630, 2008a.

[9] X.Q. Wang, A.S. Mujumdar, A review on nanofluids – Part II: Experiments and applications *Brazilian J. Chem. Engng*, 25, pp. 631-648, 2008b.

[10] K.S. Hwang, J. H. Lee, S.P. Jang, Buoyancy-driven heat transfer of water-based Al nanofluids in a rectangular cavity, *Int. J. Heat Mass Transfer*, 50, pp. 4003-4010, 2007.

[11] W. Duangthongsuk, S. Wongwises, Effect of thermophysical properties models on the predicting of the convective heat transfer coefficient for low concentration nanofluid, *Int. Commun. Heat Mass Transfer*, 35, pp. 1320–1326, 2008.

[12] V. Trisaksri, S. Wongwises, Critical review of heat transfer characteristics of nanofluids, *Renew. Sustain. Energy Rev*. 11, pp. 512-523, 2007.

[13] R.K. Tiwari, M.K. Das, Heat transfer augmentation in a two-sided lid-driven differentially heated square cavity utilizing nanofluids, *Int. J. Heat Mass Transfer*, 50, pp. 2002–2018, 2007.

[14] E. Abu-Nada, Application of nanofluids for heat transfer enhancement of separated flows encountered in a backward facing step, *Int. J. Heat Fluid Flow*, 29, pp. 242-249, 2008.

[15] H.F. Oztop, E. Abu-Nada, Numerical study of natural convection in partially heated rectangular enclosures filled with nanofluids, *Int. J. Heat Fluid Flow*, 29, pp. 1326-1336, 2008.

[16] S. Ahmad and I. Pop, Mixed convection boundary layer flow from a vertical flat plate embedded in a porous medium filled with nanofluids *Int. Comm. Heat Mass Transfer*, 37, pp. 987–991, 2010.

[17] K. Khanafer, K. Vafai and M. Lightstone, Buoyancy-driven heat transfer enhancement in a two-dimensional enclosure utilizing nanofluids, *Int. J. Heat Mass Transfer*, 46, pp. 3639-3653, 2003.

[18] M. Muthtamilselvan, P. Kandaswamy and J. Lee, Heat transfer enhancement of copper - water nanofluids in a lid-driven enclosure *Comm. Nonlinear Sci. Numer. Simul*, 15,pp. 1501-1510, 2010.

[19] H.C. Brinkman, The viscosity of concentrated suspensions and solutions, *J. Chem. Phys*, 20, pp. 571-581, 1952.

[20] T. Mahmood and J.H. Merkin. Similarity solutions in axisymmetric mixed-convection boundary-layer flow, *J. Engng. Math*, 22, pp. 73-92, 1988.

New Lower Bounds for Flow Shop Scheduling

A. Gharbi, A. Mahjoubi

***Abstract*—**The flow shop scheduling problem has become one of the most intensively investigated topics in scheduling theory. In this paper, we propose improved branch-and-bound-based lower bounds by taking advantage of the interdependence of the relaxed sub-problems. The proposed approach is assessed on two flow shop variants, namely the makespan minimization problem and the total completion time minimization problem. Preliminary computational experiments provide promising results of our improved bounds with respect to their basic versions.

***Keywords*—**Branch-and-Bound, completion time, flow shop, lower bounds, makespan, scheduling.

I. Introduction

THE flow shop scheduling problem is one of the hardest combinational optimization problems.It can be described as follows: A set J of n jobs, available at time zero, has to be processed in a shop with m machines. Each job is processed on machines M_1, M_2, …, M_m in that order. No machine can process more than one job at a time and no job preemptions are allowed. The schedule with the same job ordering on every machine is called a *permutation* schedule. The goal is to find a sequence of jobs that minimizes some criterion. Most attention has been devoted to makespan and/or total completion time minimization. The practical implications of both criteria are obvious: minimization of the makespan leads to the minimization of the total production run, and minimization of the total completion time leads to the rapid turn-around of jobs [16].

The objective of this paper is to propose new lower bounds for two variants of the permutation flow shop problem, namely the makespan minimization problem ($F|prmu|C_{max}$), and the total completion time minimization problem ($F|prmu|\sum C_j$). Both variants have been proved NP-hard if the number of machines is greater than two [5]. Many efforts have been developed to obtain optimal or near-optimal sequences, including dynamic programming [9], integer linear programming [2,24], branch-and-bound algorithms [1,3,8,11,12,15,17,21], and heuristics [7,18,22,23,27].

The remainder of the paper is structured as follows. Section II describes the framework of our proposed lower bound. Section III provides the results of our computational study.

A. Gharbi is with the Industrial Engineering Department, College of Engineering, King Saud University, PO Box 800, 11421 Riyadh, Saudi Arabia. He is also a research fellow with BEM Management School Bordeaux, France (phone:966-1-4676829; fax: 966-1-4678657; e-mail: a.gharbi@ksu.edu.sa).

A. Mahjoubi is with High Institute of Management of Tunis, Bardo, Tunisia (email: mahjoubi.amira94@yahoo.fr).

II. Framework of the Proposed Lower Bound

The quality of the lower bound is one of the most critical components of any branch and bound algorithm. Several lower bounds have been proposed in the literature for the m-machine permutation flow shop problem. The basic idea is to compute lower bounds by relaxing in different ways the constraints of this problem.

Firstly, our bounding scheme is based on the fact that if infeasibility can be stated for a relaxed problem, then it can be obviously deduced for the original one. The main steps of our procedure can be therefore described as follows:

Step 1:

Transform the m-machine permutation flow shop problem into K sub-problems. Let T denote a valid starting lower bound. Set $k = 1$.

Step 2:

Solve the feasibility sub-problem P_k using a branch-and-bound algorithm.

If there is no feasible solution with objective value less than or equal to T

Then Set $T = T + 1$and Go to Step 2.

Else

If $k < K$, then Set $k = k + 1$ and Go to Step 2.

Else Stop and Return T.

Actually, the best performing lower bounds of the literature are those based on solving the relaxed sub-problems using branch-and-bound procedures. However, a major weakness of these lower bounds consists in assuming the sub-problems as totally independent from each others. Our main contribution is to take advantage of the *inter-dependence* of the sub-problems. Indeed, if a sub-sequence of the search tree is proven not to yield feasibility for sub-problem P_k, then it will not yield any feasibility for the original problem. Therefore, there is no need to explore this sub-sequence for any other sub-problem. For that purpose, in case of feasibility, the search tree that has been developed for P_k is stored and transferred to P_{k+1} to start with. In this way, all efforts that have been made in pruning unpromising nodes will be saved. An immediate result is that some potentially feasible solutions for P_{k+1} would not be feasible any more since they have been eliminated during the tree search of previous sub-problems. Consequently, the value of the lower bound will be increased. A new search tree is only created if the addressed sub-problem is proven to be infeasible.

In the following, we provide the details of the branch-and-bound algorithm that is implemented in Step2.